Volume 2 Number 2 (September 2022)
DOI 10.24191/jaeds.v2i2.57
eISSN 2805-5756

Journal of Applied Engineering Design & Simulation

Modification of Weld Penetration Characteristics in Laser Deep Welding Using Instationary Gas Flows

B. John[1], F. Maqbool[2], D. Kowerko[3], J. Buhl[2], S. Härtel[2,*] and J. Hensel[1]
[1]Chair of Welding Engineering, Chemnitz University of Technology, Chemnitz, Germany.
[2]Chair of Hybrid Manufacturing, Brandenburg University of Technology Cottbus-Senftenberg, Cottbus, Germany.
[3]Junior Professorship of Media Computing, Chemnitz University of Technology, Chemnitz, Germany.
[*]corresponding author: sebastian.haertel@b-tu.de

ABSTRACT

The present report focuses on the integration of technology for generating temporally alternating (pulsed) gas flows in the field of laser welding. The technical realization requires specific adaptation of three core elements of the gas pulse system (valve, section of measurements, control system) to realize new parameters of laser welding. These parameters allow for a positive influence on the joining process and on the results of welding, respectively. By means of temporal control of the gas volume flow in combination with the laser welding process, it was possible to produce a force effect on the molten pool and subsequently to improve the characteristics of laser-welded seams – up to 10 % narrower, deeper at the same welding speed and laser power. The effects occurring through the use of instationary gas flow were evaluated by using the "classically" metallography and through the use of digital image processing. In parallel, the effect of pulsating gas flow on the melting zone was simulated by using specific software in order to make further statements about the effects.

Keywords: Laser welding, gas pulse, instationary gas flow, digital image processing, gas flow simulation.

Nomenclature

A	Area (mm²)
a	Distance between gas nozzle and workpiece (mm)
b	Seam width (mm)
d_{Blende}	Pinhole diameter (mm)
d_{Rohr}	Pipe diameter (mm)
d_{Spot}	Diameter of the Laser beam in focus position (mm)
E_{Blende}	Thickness of the pinhole (mm)
e	Multiplication of the deviation
f_{B}	focal length (mm)
f_{max}	Maximum deformation (mm)
f_{Puls}	Pulse frequency of the gas (Hz)
f_{zul}	Permissible deflection of the orifice (mm)
I_L	Intensity of the Laser beam ($W \cdot \text{cm}^{-2}$)
K_d	Difference coefficient
K_i	Integration coefficient
K_p	Proportional coefficient
m	Mass (kg)
P_L	Laser power (W)
p	Pressure ($N \cdot \text{mm}^{-2}$)
p_0	Line pressure (bar)
p_{N}	Seam (weld-in) depth (mm)
$p_{\text{Shield Gas}}$	Dynamic pressure of the shield gas ($N \cdot \text{mm}^{-2}$)
p_{sMax}	Maximum pressure at any point inside the keyhole ($N \cdot \text{mm}^{-2}$)
p_{upward}	Upwards vapor pressure ($N \cdot \text{mm}^{-2}$)
Q	Flow rate ($\text{l} \cdot \text{min}^{-1}$)
s	Distance (mm)
T_n	Summation of time (s)
T_v	Derivative time (s)
t	Time (s)

Received on 12.09.2022
Accepted on 18.09.2022
Published on 30.09.2022

V	Space (mm³)
$\dot{V}_{\mathrm{G}}$	Volume flow of the gas in the basic phase nozzle ($\mathrm{l} \cdot \mathrm{min}^{-1}$)
$\dot{V}_{\mathrm{P}}$	Volume flow of the gas in the pulse phase nozzle ($\mathrm{l} \cdot \mathrm{min}^{-1}$)
U_{Sensor}	Voltage signal of the sensor (V)
u	velocity ($m \cdot \mathrm{s}^{-1}$)
Δu	changes in the flow velocity of the gas ($m \cdot \mathrm{s}^{-1}$)
u_{α}	velocity of the gas before actuation of the valve ($m \cdot \mathrm{s}^{-1}$)
u_{ω}	velocity of the gas after actuation of the valve ($m \cdot \mathrm{s}^{-1}$)
v_S	Welding speed ($m \cdot \mathrm{s}^{-1}$)
y	Manipulated variable
α	Angle between gas nozzle and workpiece (°)
θ	Angle between normal vector of the surface and vector of shield gas velocity (°)
λ	Wave length of the Laser beam (nm)
ν	Shield gas velocity ($m \cdot \mathrm{s}^{-1}$)
ρ	Density ($kg \cdot \mathrm{m}^{-3}$)

Abbreviations

Laser	Light amplification by stimulated emission of radiation
VOF	Volume of fraction
VPRMAG	Constant with value between 0 and 1

1.0 INITIATION ON THE USE OF INSTATIONARY GAS FLOWS

"*The laser has become the miracle tool that science fiction authors have always believed it to be*" [1]. In particular of industrial production, the laser is not only used for cutting and joining materials, but also for generating components. Influenced by numerous setting parameters, which according to Beske [2] can be divided into four main groups (laser, machine, material and workpiece parameters – Figure 1), a wide variety of applications can be realised. From the point of view of production engineering, these four groups are narrowed down again and thus the influencing parameters are minimised. So it is only possible via laser and machine parameters to influence the achievable results. The other way around means that if these parameters are expanded, the possibilities for influencing will improve.

The development of technology for temporal modification of process-specific gas flows during gas-shielded welding [3] provided the user with additional influencing parameters, such as the gas volume flow in the pulse ($\dot{V}_{\mathrm{P}}$) and basic phase ($\dot{V}_{\mathrm{G}}$) or the pulse frequency (f_{Puls}). Based on the use of the three core elements (actuator, measuring section and control), it is possible to manipulate the molten bath and its movement by means of gas pulses and thus cause an increase in the joining speed, the weld penetration characteristics and an improvement with regard to the formation of the seam structure.

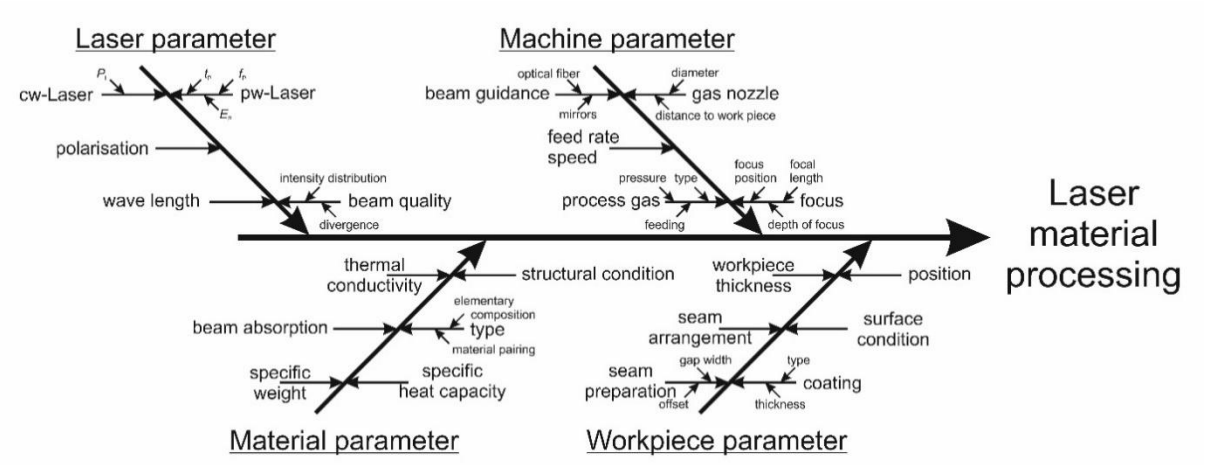

Figure 1. Parameters influencing laser material processing according to [2]

The work of Ebert [3] and John [4] took up these process advantages and transferred them to further joining application areas such as plasma powder welding and laser welding. In the case of the latter in particular, this was

accompanied by a complete revision of the established system with regard to the significantly changed boundary conditions of the process, higher dynamics as compared to classic arc process. Based on the findings and technology development on the part of Thurner [3], numerous modifications were made to the system. The basic concept was retained, but the core elements were adapted in their expansion stages to the new boundary conditions. This can be summarised in the modification of the technical setup to increase the pulse frequency from $f_{\mathrm{Puls}} < 30$ Hz to $f_{\mathrm{Puls}} > 300$ Hz. But at the end, there is the question that how these changes influence the weld penetration characteristics of laser deep welding and which benefits come along.

2.0 THE GASE PULSE TECHNOLOGY – STATE OF THE ART

2.1 Modifications of the core elements

2.1.1. Actuator

As part of the adaptation of the actuator to the new conditions, the valve was replaced. A proportional directional control valve (MPYE from Festo) in spool design with minimal leakage was used to implement the more switching-intensive applications.

A plunger drive acts directly on the valve spool and thus realises its exact positioning. Accordingly, precise flow rates can be set based on discrete opening states. At the same time, the gate positions are monitored by an integrated sensor and adjusted via the internal valve electronics. As a result, better static as well as dynamic valve characteristics can be implemented. The switching hysteresis of the valve between opening and closing is also significantly improved compared to the proportional valves used previously, which in turn makes it possible to set any volume flow regardless of the direction of movement of the slide.

However, the use of the new valve type does not achieve all the desired goals; in particular, pulse frequencies of $f_{\mathrm{Puls}} > 300$ Hz were not feasible. In addition to line-internal discontinuities – such as changes in line diameter, deflections etc. – as well as due to a large distance between the actuator and the effective zone of the pulse (melt pool), valves operated close to their cut-off frequency also cause the pulse to destroy. Consequently, the design of the gas pulse system is extended to include a fast-switching valve (MHJ from Festo), which allows pulse frequencies of up to almost 1000 Hz. Thus, the field of application of the technology could be expanded to include laser-related cutting and joining tasks.

Another advantage is reflected in the compact and weight-reduced design of the fast-switching valve, which has made it possible to significantly reduce the distance between pulse generation and the effective zone of the pulse (melt pool).

At the same time, however, attention has focused to the switching states of the fast-switching valve, as this can only realise two discrete states (open or closed). As a result, exact control of the volume flow between any maximum and minimum can no longer be implemented. This means the realisation of $\dot{V}_{\mathrm{G,min}}$ or $\dot{V}_{\mathrm{P,min}} \neq 0$ l·min^{-1} is not possible.

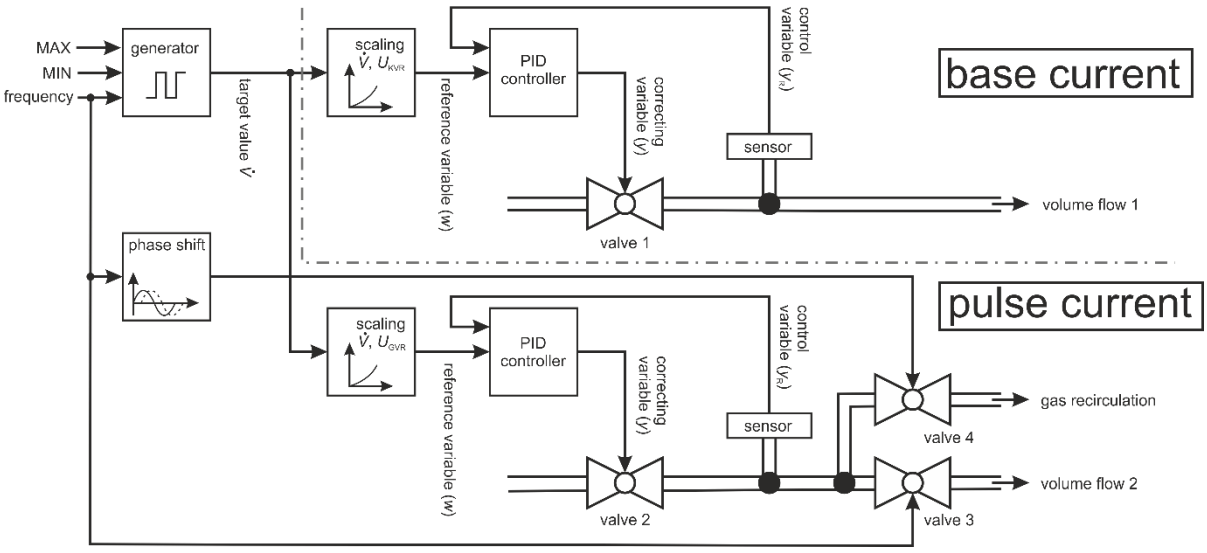

Figure 2. Schematic representation of the further developed control loop for gas pulsing in laser material processing using a base and pulse current segment.

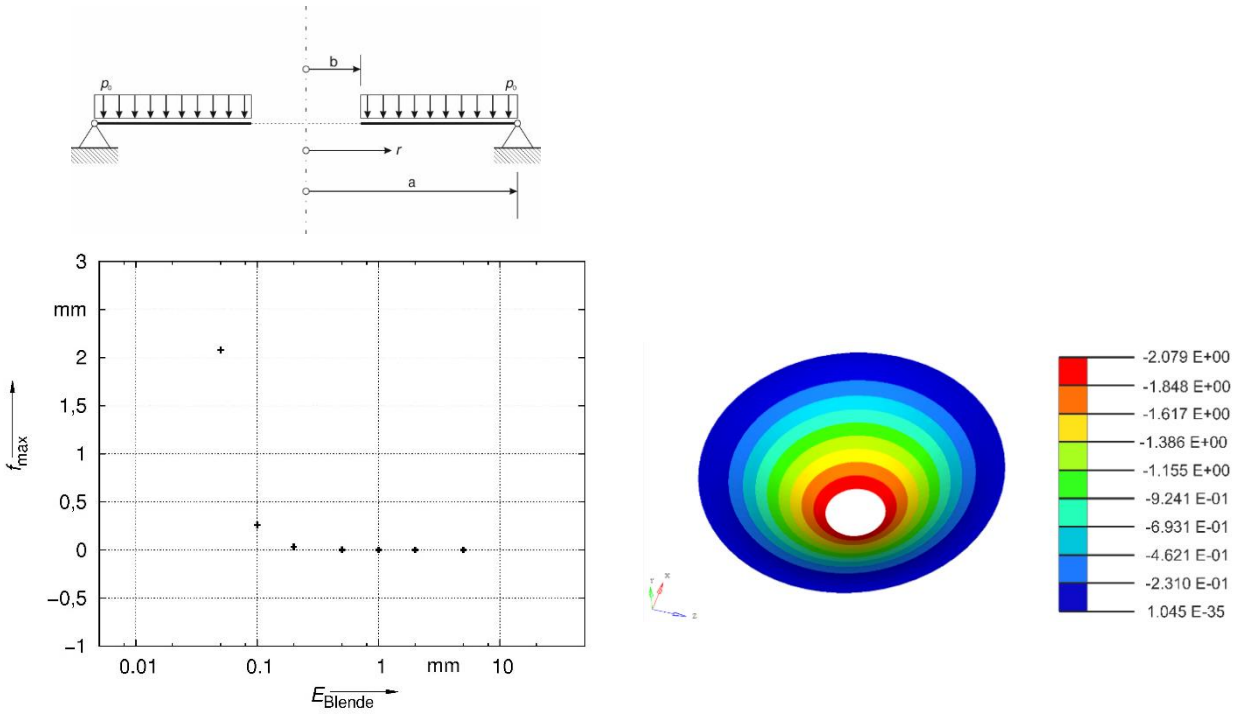

(a) (b)

Figure 3. a) Simulation of the maximum deformation ($f_{\max}$) of the pinhole geometry depending on different material thickness of the pinhole (E_{Blende}) according to Mathiak [7] – boundary conditions: $p_0 = 5$ bar; $2a = d_{\text{Rohr}} = 10$ mm; $2b = d_{\text{Blende}} = 2$ mm; b) one result of simulated deflection of a pinhole – material thicknesses E_{Blende} = 0.05 mm

In order to counteract this technical effect, the basic and the pulse volume flow are divided into two different strings, which only unite in the gas nozzle. A separate measuring system and a separate actuator are integrated for each string. All of these are also integrated in the control system. This is illustrated in the schematic diagram of the further developed control loop in Figure 2.

This diagram also shows that, in addition to the measuring equipment and the two valves (valve 2 [MPYE] and valve 3 [MHJ]), the string for the pulse current phase has another valve with the number 4. This is also an MHJ fast-switching valve.

The technical background of this step can be explained by the fact that sudden changes in the flow velocity ($\Delta u = u_\alpha - u_\omega$)[A] as a result of a high-frequency opening or closing of valve number 3 cause dynamic pressure to change (pressure surges, $\Delta p_{Stoss} = c\rho\Delta u$ taking into account the medium density ρ and the wave propagation velocity c) and thus cause a high dynamic mechanical load on all components within the pipe system.

It can be assumed that the pressure surge refers to both the increase ($u_\alpha > u_\omega$) and the decrease ($u_\alpha < u_\omega$) of the pressure in the pipe system. Although the effects caused by the pressure surge are minimised by the elasticity of the hose wall and the compressibility of the flowing medium, a clearly measurable, constantly changing pressure fluctuation nevertheless occurs. This alternating pressure fluctuation moves with the period $2t_{\text{refl}}$[B] through the inside of the pipe and has its origin in the conversion of the kinetic energy of the flowing medium into deformation work [6].

Although there is a decrease in the pressure fluctuations caused by friction (fluid and pipe wall friction), it is only to a small extent due to a negligible energy transfer. Thus, it can be assumed that such pressure surges move almost undiminished and with almost the speed of sound through the pipe system. Or in other words, the pressure conditions change permanently in a short time sequence. The resulting pressure fluctuations are also detected by the measuring section of the volume flow, which influences the measured values and also the control of the system. This results in an overshooting of the control loop, since the falsification of the measurements of the prevailing volume flow is so strong that a sensible control of the gas pulse system is difficult to implement or rather impossible.

[A] $u_\alpha \triangleq$ velocity before and $u_\omega \triangleq$ velocity after actuation of the valve

[B] $t_{\text{refl}} \triangleq$ reflection time in which the pressure wave originating from the valve hits the shut-off device again after passing through the string once.

To counteract these effects, the gas in the pulse flow string is divided into two equal flows again, after it has passed the measuring system. Both are switched via a separate fast-switching valve, whereby there is a time offset

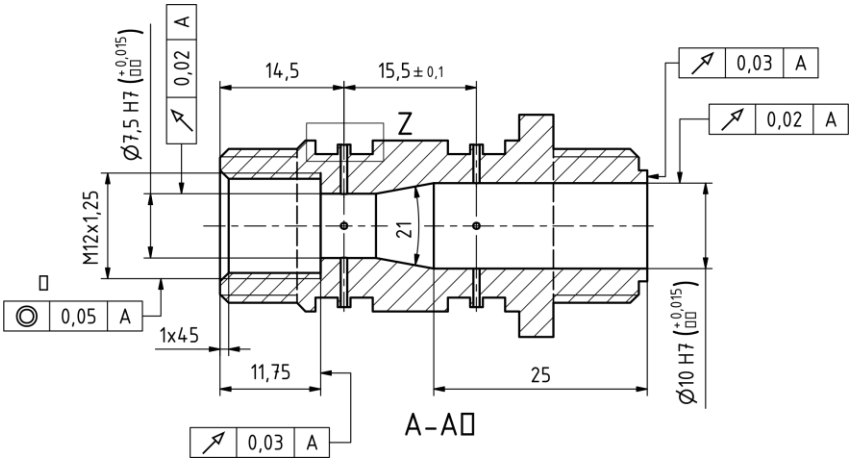

Figure 4. Schematic structure of a Venturi tube for the creation of differential pressures

between the activation of the valves. In this way, valve 3 opens and closes exactly half a period out of phase with valve 4. This makes it possible to achieve a constant flow rate of the medium in the string and thus more stable measurements and, conversely, more stable control of the system.

2.1.2. Measuring section

The measuring section, which is integrated into the string system, records the control deviation of the reference variable via an integrated measuring sensor. This sensor measures a pressure difference, which is generated for a short time due to the construction of the measuring section, and passes it to the control unite as a voltage signal. The basis for this is DIN EN ISO 5167 [8] which is a standard for recording flow rates in fully flowed pipelines. In addition of changing the valve type and its integration sequence, it is also imperative to adapt the measuring device for recording the volume flows in the strings ($\dot{V}$). The principle of a pinhole as a throttle element for generating a short-term pressure difference based on DIN EN ISO 5167 Part 2 appeared unsuitable with regard to the pipe diameters of the gas supply, which was used in laser material processing ($d_{\mathrm{Rohr}} \leq 10$ mm), and the pressures prevailing in them.

The values of the individual form elements of the orifice specified in the standard and thus their constructive design depending on d_{Rohr} are difficult to implement in terms of production technology – so the material thickness of the orifice (E_{Blende}) ranges from 0.05 mm to 0.5 mm. In the simulative consideration of this point and taking into account a standard prevailing line pressure of approx. $p_0 = 5$ bar, the deflection of the orifice f_{zul} =0.0025· (d_{Rohr}) specified by the standard cannot be observed either – see Figure 3.
Futhermore strong turbulences occur within the flow before and after the throttle element, which negatively influence the recording of the measured values to a high degree and consequently make the control of the system more difficult.

The pressure difference is now generated in accordance with DIN EN ISO 5167 Part 4. Now using a Venturi tube, it is integrated into the pipe system. Above an inlet cylinder, which merges into an inlet cone and then tapers to a cylindrical neck section before returning to the initial diameter of the pipe via a defined length of conical diffuser, the Venturi tube (see Figure 4) forces a change in the dynamic pressure component of the gas flow. At the same time, the pressures upstream of the inlet cone and in the neck section of the pipe are recorded, allowing to determine the pressure difference between these two points.

In this way, the established measurement principle follows the fluid mechanical approach of Bernoulli's equation (law of conservation of energy) using the continuity equation (law of conservation of mass). The starting point is the assumption that a mass (δm_1) is transported through a space ($V = \delta s \cdot A$) within a specific time interval (δt). At the same time, due to the law of conservation of mass, another mass (δm_2) must leave this space – formula (1) and (2).

$$\delta m_1 = \delta m_2 \tag{1}$$

$$\rho_1 \cdot \delta s_1 \cdot A_1 = \rho_2 \cdot \delta s_2 \cdot A_2 \tag{2}$$

The mass transported per time is defined as mass flow ($\dot{m} = \frac{\delta m}{\delta t}$) and from this, the continuity equation can be derived (formula (3) with $u = \frac{\delta s}{\delta t}$).

$$\dot{m} = \rho_i \cdot \dot{V}_i \qquad \text{mit} \qquad \dot{V} = u \cdot A \qquad (3)$$

It can be assumed that the volume flows within the laser material processing are below 40 l·min^{-1} ; therefore, the used gases can be described as incompressible. Consequently, the density of the gases can be regarded as a constant, which leads to a simplification of formula (3) to formula (4).

$$\dot{V} = u_1 \cdot A_1 = u_2 \cdot A_2 \qquad (4)$$

Under this assumption, the pressure difference can now be determined by using Bernoulli's equation. This system of equation consists of three terms; the pressure energy (static pressure), the kinetic energy (dynamic pressure) and the potential energy (geodetic pressure). From this fact and from the assumption that the proportion of the geodesic pressure goes towards zero, Equation (5) can be derived to describe the pressure differences between two points.

$$p_1 + \frac{\rho}{2} u_1^2 = p_2 + \frac{\rho}{2} u_2^2 = \text{constant} \qquad (5)$$

Inside the measuring system, the caused pressure difference is recorded via the pressure tapping points on the Venturi tube using a calibrated and temperature-compensated pressure measuring sensor. A voltage signal is passed to the control and regulating section of the system without any time delay. The sensor works according to the piezoresistive measuring principle, whereby four resistors on a silicon diaphragm are connected together to form a measuring bridge, so that a pressure-dependent deformation of the diaphragm causes a change in the electrical voltage. The resulting voltage signal (U_{Sensor}) precisely reflects the possible change in the volume flow.

2.1.3. Control unit

The further processing of the voltage signal (U_{Sensor}) is done with a corresponding control loop whose tasks can be divided into three categories:

- generate,
- detect,
- regulate.

The system as such consists of an industrial PC with integrated measuring card and the system design software "LabVIEW" for the simulation of electrical components or complete circuits. With this software, data can be acquired and control loops can be operated. So it is possible to record the data of the pressure sensors via the connected measuring card (input channels) in a predefined frequency, to process it internally in the computer (actual-target comparison) and to return specific control signals via the output channels of the measuring card to the actuators – in this case the valves. The corresponding control algorithm is completely redesigned and programmed to meet the new technical boundary conditions – type and number of to be controlled valves as well as reading out and processing the incoming voltage signals from the measuring sensors.
The central element of the control loop is a combination of three different types of controllers, which are within a few milliseconds:

- detect the flow velocity in the pipe system (query actual state),
- determine the deviation from the setpoint (actual-target comparison) and
- vary the manipulated variable so that the deviation from the setpoint is minimised.

The solution to such a technical challenge is achieved by combining proportional, integrating and differentiating components within a controller - a proportional-integral-differential (PID) controller.
The proportional part of this system enables a continuous manipulated variable (y) in a fast reaction, which, however, is accompanied by a permanent control deviation due to the multiplication of the deviation (e) with the proportional coefficient (K_p) [9] [10].

This is contrasted by the integral part of the controller. It reduces the permanent control deviation as far as possible, but shows a delayed reaction due to the summation of e over time (T_n). The whole thing is to be seen in connection with the multiplication of this sum with the specific integration coefficient ($K_i = \frac{K_p}{T_n}$) [9]. Thus, the step response depends on T_n and provides an increasing inertia of the system. This means, the smaller T_n, the faster the control signal reacts. However, this is accompanied by an oscillation of the control loop, at the end of which is a completely unstable behaviour of the system.

With the help of the differential component, these effects can be counteracted; the oscillations within the transient process of the control loop are prevented by evaluating the control deviation and calculating the rate of change. This result is multiplied by the difference coefficient ($K_d = K_p \cdot T_v$; proportional coefficient multiplied with derivative time). Based on these three variables, the formula (6) for the manipulated variable y with the

specific weighted coefficients for the respective proportions is obtained in summary. By combining the different controller types in this way, the disadvantages of individual control elements can be compensated and the control unit can be optimised.

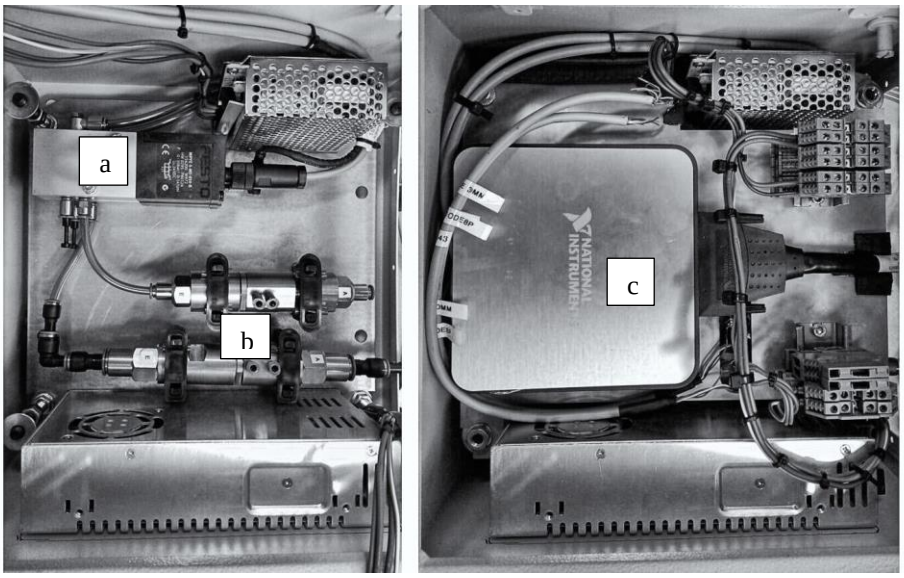

Figure 5. in-box-design of the gas pulse system – a) actuator (valve); b) measuring section (Venturi tube); c) control unit

$$y(t) = K_{\mathrm{p}} \cdot e(t) + K_{\mathrm{i}} \int_0^t e(t)\delta t + K_{\mathrm{d}} \frac{\delta e(t)}{\delta t} \qquad (6)$$

Firstly, the control unit generates a time constant and starts converting the specified volume flows within the basic or main flow phase into voltage signals (setpoint values) by using specific mathematical correlations. At the same time, the control system includes the voltage signals from the measuring section (actual values) – i.e., the currently prevailing volume flows in the pipe system – in the further calculations and stores this for a later evaluation of the research results. Now it is possible to derive control deviations from the actual-target comparison of a temporal control run (A). These values are transferred as error variables to the subsequent control run (B) and also added up by using the formula (6) and furthermore subtracted from the manipulated variables from run A. This sum is transferred as a new manipulated variable to the control system. At the same time, the control system generates a freely selectable voltage signal in the background to control the fast-switching valves.

The further development of gas pulse technology, shifting away from the modular design to a compact gas control unit as an in-box-design (see Figure 5) for integration into different laser processing systems, provides the user with new parameter variables in influencing laser material processing. In addition to the pulse frequency (f_{Puls}), they inlcude the volume flows in the pulse phase ($\dot{V}_{\mathrm{P}}$) and the base current phase ($\dot{V}_{\mathrm{G}}$) as well as the switching ratio between the phases (e. g. 50 %) and the shape of the pulse (square, sawtooth, sinusoidal pulse etc.). With those separate setting, specific changes in the processing result can be achieved.

2.2 Hypothesis

The motivation for the further development of gas powder technology and its transfer from the field of arc processes to beam technology production is the effects occurring in the melt pool respectively in the movement of the melt pool. The greatest possible influence through an induced movement as a result of a temporal change in the volume flow of the process gas takes place on particularly "small" melt pools [4]. This is realised by mechanically influencing the process gases inside the feeding system in order to exert a force on the melt pool with a targeted gas pulse in correspondence with the laser process.

Thus, this technology provides the user with further (machine) parameters for achieving improved joints. It can improve specific effects such as the reachable penetration depth or the formation of the microstructure.

By using a pulsating shielding gas, it should be possible to increase the welding speed without increasing the energy per unit leng. So the penetration depth will still be the same [11] because the targeted orientation of the molten pool flow, laminar or turbulent, brings about changes in the seam shape and the seam structure. This alludes to the influence of convection, which sets in from a penetration depth of the process into the material of around 0.5 mm in the liquid phase and causes temperature and concentration differences. Due to the permanent modification of the surface tension of the melt, other weld penetration characteristics – wider or deeper seams – can be achieved.

Another field of application in laser material processing for this technology is the surface modification of materials – remelting or alloying by laser. The modification of the gas volume flow enables the generation of an artificial melt pool movement [4], which can realise an improvement of the structure of the wedled seam. Looking at the behaviour of the melt during cooling, it becomes apparent that the solidification processes have a decisive influence on the subsequent mechanical-technological properties of the joined products. Crystal growth starts at the solidification front and proceeds in the opposite direction of the heat flow. The solidification morphology of the resulting structures depends on the cooling rate, the temperature gradient and the local solidification speed. The cooling rate in turn results, for example, as the product of the feed rate and the temperature gradient in the feed direction. As a result of an increasing cooling rate, a finer microstructure is achieved.

According to Ebert [4], at the growing crystals, the local temperatures constantly change due to the generated movements in the melt pool – dendrites break off from the growing crystal and in turn to a new basis for crystal growth. This effect, as implied by the user, forms the basis for finer microstructures and consequently better mechanical-technological properties within the joining zone.

3.0 EXPERIMENTAL INVESTIGATIONS

3.1 Welding

The test welds took place on the modular laser processing centre "microWELD" from 3D-MICROMAC AG after the integration of the in-box-version of the gas pulse technology. This machine has the largest possible number of degrees of freedom for the creation of welded joints with regard to both industrial and scientific investigations. This machine variant shows its advantages in the high positioning and repetition accuracy of less than unter 10 µm at speeds greater than $1\ \mathrm{m \cdot s^{-1}}$. Depending on the type of application, the system itself can be equipped with a fixed optic of coaxial or lateral gas feed (f_B = 250 mm; $d_{Spot} \leq 100$ µm), as used in this case, or a scanner system (working field of 250 mm x 250 mm; f_B = 470 mm). The beam source used in the investigations is a single-mode fibre laser source (λ = 1064 nm) from IPG Photonics with laser power (P_L) up to 1 kW.

The investigation of the influence on the seam geometry and the effects caused by a transient process gas flow are the focus of the test series. The main objective is the derivation of corresponding parameters for a positive modification of the joining process with regard to the welding speed and the seam shape (seam surface, welding depth, seam width etc.).

Starting from a central parameter set, only one setting variable is modified to varying degrees and its effect on the welding result is documented. The used basic parameter set, which is defined by a total of eight variables, is composed as follows:

- the angle between nozzle and workpiece (α),
- the distance between nozzle and workpiece (a),
- the volume flow of the process gas, divided into pulse phase ($\dot{V}_P$) and base flow phase ($\dot{V}_G$),
- the pulse frequency (f_{Puls}),
- the percentage laser power (P_L),
- the feed rate (v_S) as well as
- the direction of movement of the nozzle during the process (trailing or leading).

At the same time, the welding result of the test series, which is using the gas pulse technology, is compared to the result of an unpulsed welding process (named reference parameters) with almost similar parameters (α = 45°, a = 3 mm, $\dot{V} = 5\ \mathrm{l \cdot min^{-1}}$, P_L = 50 %, v_S = 15 $\mathrm{mm \cdot s^{-1}}$, trailing or leading). On one hand, this should make it possible to compare the effect of stationary and instationary shielding gas flow on the welding process. On the other hand, the effect on the joining process should be clarified by varying the "new" parameters. A high-alloy stainless steel (X5CrNi 18-10; material number: 1.4301) with a material thickness of t_B = 10 mm is chosen as a suitable base material for the investigations; and argon is used as shielding gas.

The analyses of the individual weld samples included the evaluation of weld seams via the recordings of the surface structure and metallography as well as a new approach, which uses digital image processing of high-speed video recordings, to make statements about the process and the effect of the different parameters over a defined period of time.

3.2 Digital image processing

The recordings for the high-speed video analysis are realized with the help of a camera (Vision Research Phantom v310) integrated into the machine room. The camera allows a maximum frame rate depending on the resolution of up to 500,000 fps. In combination with the exposure system from Cavitar Ltd, accurate process recordings could be determined in a time interval of 500 µs. This made the base for analysis.

The objective of the image processing algorithm developed is to quantitatively determine the geometry of the melting zone during the welding process in order to subsequently correlate it with the basic parameters of the welding process mentioned above. To a good approximation, the projection of the 3-dimensional melt zone onto

the camera sensor can be approximated with an ellipse. Figure 6 and Figure 7 show ellipse parameters such as the ellipse center and the ellipse area, respectively, as a function of location and time.

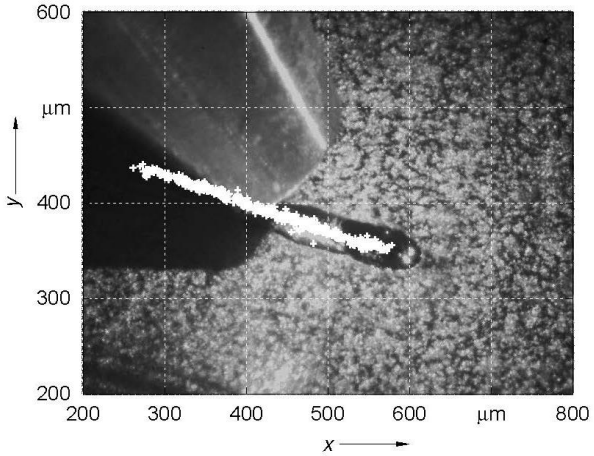

Figure 6. Progress of the ellipse centre of the molten bath over time or over the image sequence using a selected example – α = 45°; a = 3 mm; $\dot{V}_P = 5\ l \cdot min^{-1}$; $\dot{V}_G = 0\ l \cdot min^{-1}$; $f_{Puls} = 100\ Hz$; $P_\mathrm{L} = 50\ \%$; $v_\mathrm{S} = 15\ mm \cdot s^{-1}$; trailing

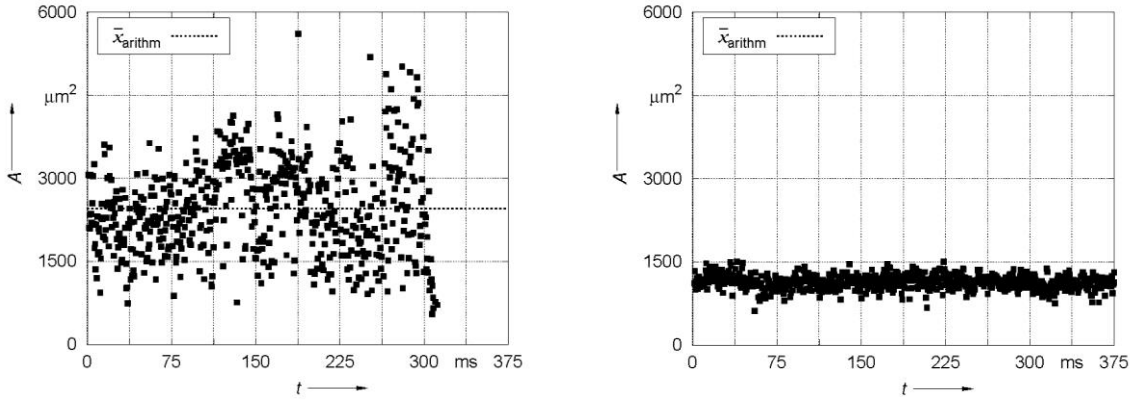

Figure 7. Comparison of the image processing analysis with regard to the effect of the protective gas on the size of the ellipse area of the melt zone during the process using the parameter set without gas pulse (a) or with gas pulse (b).

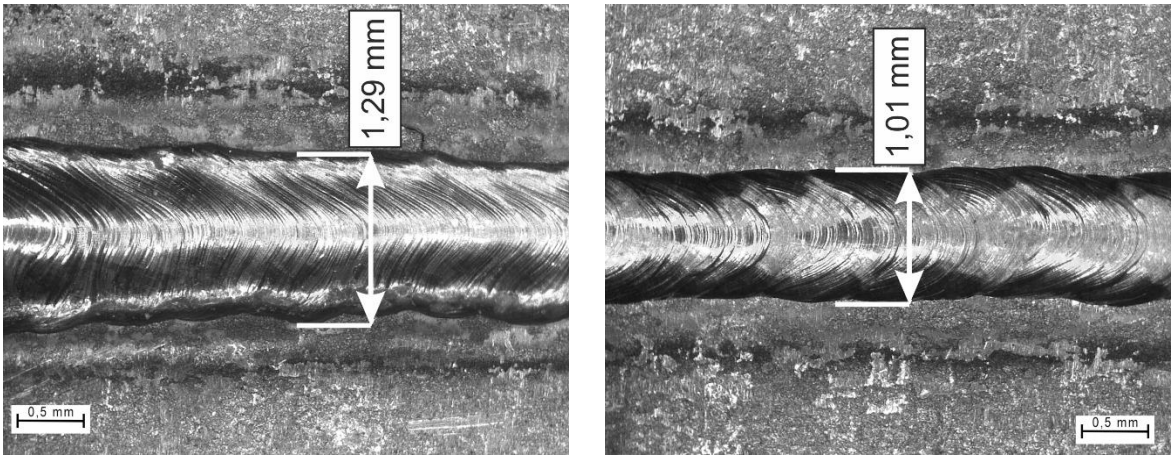

Figure 8. Representation of the results of the measurement of the seam width at the seam surface using the parameter set without gas pulse (a) and with gas pulse (b).

The requirements for the image analysis are high due to the high noise component of the signal, as well as the relatively small spatial melt pool zone. The underlying algorithm is presented in [12] [13]. It is an image processing chain combining classical image processing operators. Different images of neighboring video frames, smoothing, edge detection, morphological operators, and contour detection are used (some multiple times).

In combination with heuristically found threshold values, the ellipses could be fitted as envelopes around the melting zone at each time step. The ellipse is mathematically described by a short and a long semi-axis, their angles with respect to the horizontal image axis and the ellipse center (x, y). Figure 6 shows that the ellipse center does not follow the rectilinear trajectory of the weld, but fluctuates around it in time/space. To some extent, this is due to the aforementioned image noise, but also to the process parameter-dependent dynamics of the welding process itself, which markedly affects the shape of the fusion zone. As can be seen in Figure 7, the noise of the ellipse area content is significantly increased when the gas flow is pulsed, as can be seen from the higher amplitudes. In [12], an approximately linear relationship between laser power and ellipse area is also found. To investigate the influence of the gas pulse frequency on the melt zone geometry in more detail, further research is needed under optimized recording conditions (e. g., closer to the melt zone, variation of exposure and perspective). A temporal synchronization between video and gas pulse would allow concrete impulse response function analyses and thus the immediate spatial response of the melt zone to the gas pulse.

3.3 Numerical model of welding and its set-up

Alongside experimental investigations, numerical simulations of the welding process are developed using the commercial software Flow3D®. The main focus of the simulations is to validate the experimental investigation and show that the shielding gas flow can considerably affect the weld seam and shape during a welding process. In this regard, two different simulation models are developed. All the process parameters are kept constant similar to that of the experiments including laser velocity, material, as well as laser power. The only difference between the two numerical models is the shield gas flow, i.e., with and without shield gas. A brief description of the mathematical formulation used for the numerical model is presented. The code in Flow3D® is based on the volume of fraction (VOF) method.

During the process of welding, the shield gas is injected. In the case of Flow3D®, the shield gas flow is modeled by a dynamic pressure being applied on the surface of the metal without actually introducing the shield gas as a separate fluid in the numerical simulation. The mathematical description of the dynamic pressure replicating the shield gas effect ($p_{\text{Shield Gas}}$) is as follows.

$$p_{\text{Shield Gas}} = \frac{1}{2}\,\rho v^2 \cos\theta \qquad (7)$$

ρ represents the shield gas density, v is the shield gas velocity and θ is the angle between the normal vector of surface and vector of shield gas velocity. As Argon is used as a shielding gas in the experimental investigations, the density of the Argon and its velocity in the Z-direction, i.e., is given as input for the numerical simulations to model the shield gas effects. The density of Argon is $1.784 \cdot 10^{-3}$ g $\cdot$ m^{-3}, whereas the velocity of the shield gas is calculated according to the Equation (10). For 30 $l \cdot min^{-1}$ flow rate, the velocity of the shield gas is 0.75 m $\cdot$ s^{-1}.

The reaction force caused by the rapidly expanding gas due to evaporation at the melt pool interface must be considered for an accurate description of the deep penetration welding. This is also referred to as evaporation pressure. This reaction force is modeled by applying pressure at the interface during evaporation. The evaporation pressure is of high significance when the energy density is high. The mathematical formulation is as follows:

$$p = A \exp\left\{B\left(1 - \frac{T_{\text{v}}}{T}\right)\right\} \qquad (8)$$

p and T_{v} represent the evaporation pressure and saturation temperature respectively. T is the temperature and A and B are the equation constants. Based on the selected material, in the current case of steel (1.4301), the saturation temperature is available in the selected material model built-in in the Flow3D® software, and parameters A and B are automatically calculated by the Flow3D®.

In addition to the modeling of shield gas and evaporation pressure, rising gas due to melting and evaporation of the base metal at the bottom of the keyhole should also be considered. The effect of the rising gas is introduced in the numerical model by the following equation:

$$p_{\text{upward}} = p_{\text{sMax}} VPRMAG \|\cos\theta\| \qquad (9)$$

p_{upward} is the upwards vapor pressure and p_{sMax} is the maximum pressure at any point inside the keyhole and is constantly taken as input from the numerical model during each calculation step to calculate the upward vapor pressure. θ is the angle between the free surface and the upward vapor direction. *VPRMAG* is a constant with a

value between 0 and 1 and represents the multiplier of maximum pressure. As the maximum pressure is taken from the keyhole in order to have an average effect of the whole pressure inside the keyhole, a scaling effect of *VPRMAG* is used, so that the upward vapour pressure is always smaller than the maximum pressure inside the keyhole. For the current simulation, a value of 0.2 is used. At the same time, the multiple laser reflection option is also activated for the numerical simulations.

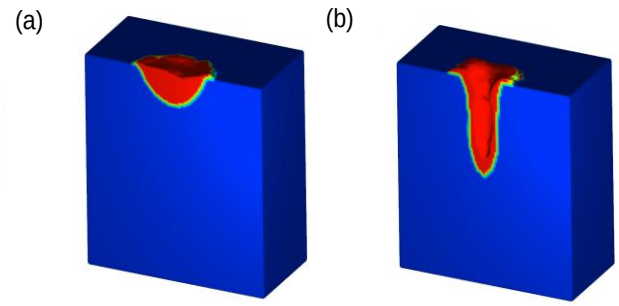

Figure 9. Melt pool profile (a) without evaporation and laser reflection and (b) with evaporation and laser reflection

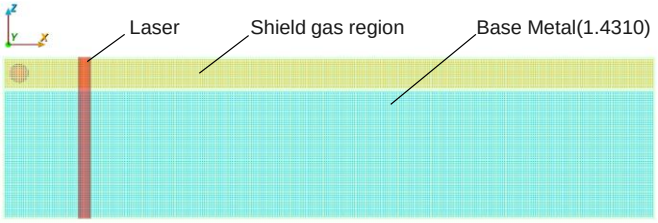

Figure 10. Set-up of the numerical model

When a keyhole occurs due to deep penetration welding, the laser gets reflected inside the keyhole and causes further irradiation. This continuous process causes a lower energy density at the end of the keyhole. Hence, this causes the keyhole to become deep and sharp. This effect is activated by changing the multiple reflection option and using the angle-dependent ($\cos\theta$) option. This option controls the angular dependence of absorption rate.

In order to accurately capture the weld pool profile, it is necessary to take into consideration the above-reported phenomenon. In order to demonstrate this, in the initial step, a static simulation where the laser source does not move is performed. For one case, the above-reported phenomenon is not modeled, whereas, for the second case, they are taken into consideration. The melt pool profile for both cases is presented in Figure 9. It can be seen that the melt pool profile is completely different for both cases. In the case of Figure 9(b), the melt pool profile matches the experimental melt pool profiles in terms of shape and geometry. Hence, it can be concluded that to accurately model the melt pool profile and laser welding, it is necessary to take into consideration the phenomena such as laser reflection and evaporation.

A numerical model of laser welding similar to that of the experiments is developed by taking into consideration all the above-reported phenomena. As the main focus is on the effect of the shield gas, two different numerical models are used to replicate the experimental set-up. However, in one case, the shield gas is modeled and in another, it is not modeled. A brief introduction of the model set-up in Flow3D® is presented followed by the results. A separate module from Flow3D® referred to as Flow3D-Weld is used to set up the welding parameters for the numerical model. The numerical model is presented in Figure 10. Two different cell blocks are modeled. The first block represents the base metal, whereas the second block represents the atmospheric conditions and the shield gas region, where dynamic pressure due to shield gas is applied. The total length of the sample in the X-direction is 60 mm. A laser power of 500 W is used. The laser source moves along the x-axis at a velocity of $15\ \mathrm{mm}\cdot\mathrm{s}^{-1}$, whereas Argon is used as the shield gas. In Flow3D-Weld, the input for modeling the shield gas flow is the gas density and the velocity. In order to convert the flow rate from the experiments into velocity, the volume flow rate equation is used. The equation is described as

$$Q = v \cdot A \tag{10}$$

Q represents the volume flow rate, *v* is the velocity of shield gas and *A* is the area of the nozzle diameter. The diameter of the shield gas nozzle varies between 1.0 mm to 2.5 mm. Therefore, a mean value of 2.0 mm is used for calculating the velocity to be the input of the numerical model. In this regard, a numerical model with shield gas at a flow rate of $30\ \mathrm{l}\cdot\mathrm{min}^{-1}$ and without shield gas flow, i.e., $0\ \mathrm{l}\cdot\mathrm{min}^{-1}$ is developed. The simulations are

run for a total time of 6 s. The laser welding is carried out in the first 3 s and in the last 3 s while the sample cooling takes place. The results from the numerical model are presented in Figure 11, which indicate that with an increased shield gas flow rate, a significant difference in the weld seam width is achieved. The experimental observation indicates that if the shield gas flow is within a certain limit, i.e., around $10\,\mathrm{l}\cdot\mathrm{min}^{-1}$, it can have a positive effect on the weld seam. In the case of a higher flow rate, the excessive flow rate of the shield gas will have a negative impact on the weld seam profile. This is due to the fact that a significant amount of the molten metal is blown out of the melt pool. This effect only becomes evident when the flow rate is higher than around $15\,\mathrm{l}\cdot\mathrm{min}^{-1}$. Hence, two numerical models without and with shield gas by taking a higher flow rate of $30\,\mathrm{l}\cdot\mathrm{min}^{-1}$ are used to demonstrate this fact.

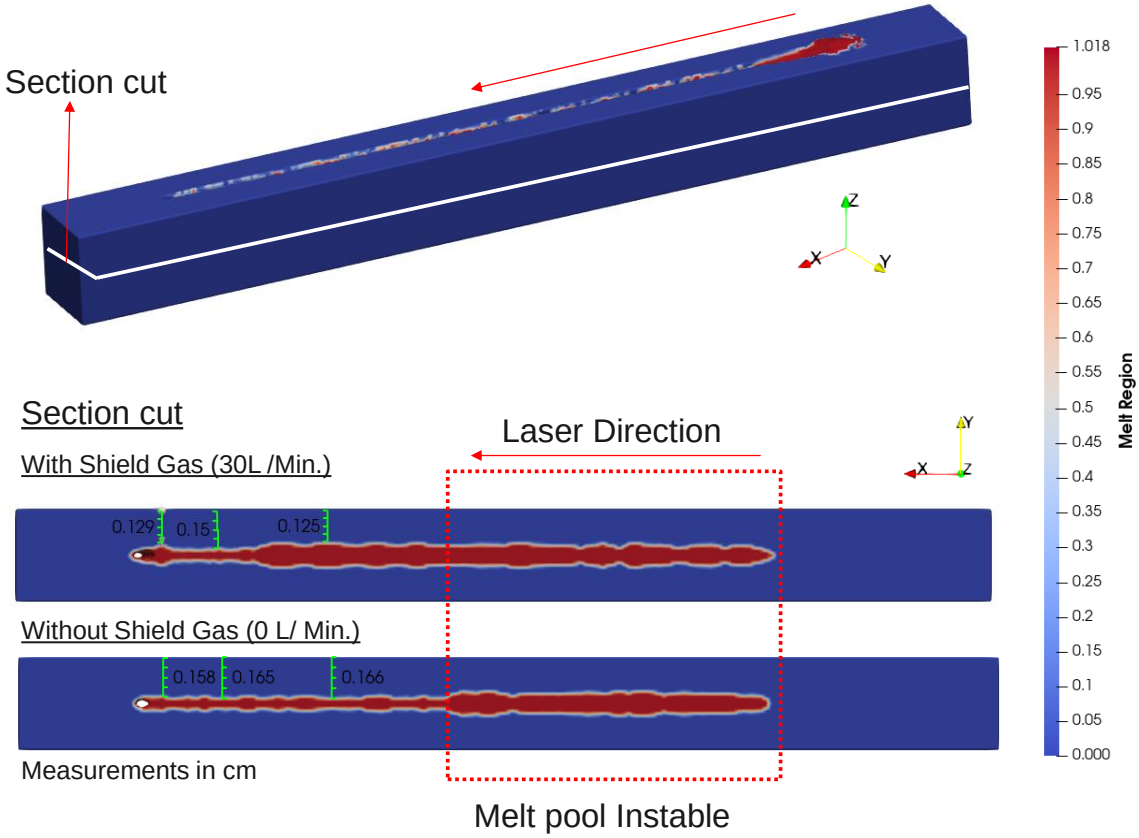

(a)

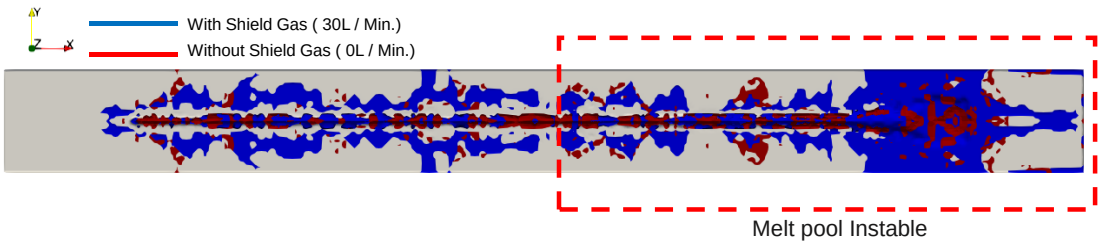

(b)

Figure 11. Blown out molten metal from the melt pool (a) with shield gas (b) without shield gas

A section cut was placed at the middle of the specimen as shown in Figure 11(a). The weld seam is analysed along this section for the two numerical models, i.e., with and without shield gas. It is important to consider that the melt pool can be divided into a stable and unstable regions. As soon as the laser welding process begins, the melt pool achieves a stable state over a certain distance. At this distance, the melt pool has been marked as unstable. The comparison of the weld seam has been carried out in regions where the melt pool is stable. The distance of the weld seam to the sample outer walls is marked in Figure 11(a).

A higher flow rate causes a blowout of the molten metal from the melt pool. As a consequence, the width of the weld seam is considerably higher for the nuermical model with shield gas as compared to the numerical model without shield gas. Numerical results agree with the experimental observation.

In order to better demonstrate the effect of the shield gas in blowing out the molten metal from the melt pool, Figure 11(b) is presented. The figure presents the top view of the specimen with blown-out metal from the melt pool. Figure 11(b) represents artifacts that are stored as scalars during the numerical simulation as the laser follows its path. In this case, they represent the molten metal that is ejected from the melt pool. The comparison shows a higher number of artifacts for numerical model with shield gas, hence validating that a higher amount of molten metal is blown out of the melt pool, which in turn affects the height and width of the weld seam.

3.4 Results

The metallographic analysis of the results showed that the samples produced with a instationary gas flow had increased weld widths and depths compared to the results of welded samples using a stationary gas flow of $\dot{V} = 5\ \mathrm{l{\cdot}min^{-1}}$. At the same time, the instationary flow ensured an equalisation of the weld penetration characteristics with trailing or leading shielding gas nozzle. This is described by the aspect ratio of seam (weld-in) depth (p_N) to seam width (b).

Depending on the orientation of the nozzle, the delta of $\frac{p_\mathrm{N}}{b}$ is still 0.7[C] for the parameter set without gas pulse. This value decreases by approx. 67 % to 0.23 during the investigations when using the instationary gas flow ($\dot{V}_P = 5\ \mathrm{l{\cdot}min^{-1}}$; $\dot{V}_G = 0\ \mathrm{l{\cdot}min^{-1}}$; $f_\mathrm{Puls} = 100\ \mathrm{Hz}$). This means that when using gas powder technology in relation to the position of the shielding gas nozzle, there is either a significant increase in the seam depth or a decrease in the seam width. Thus, this changes the result of the aspect ratio.

In fact, it is primarily the welding depth that seems to change. It experiences a significant increase due to the instationary gas flow, which is particularly the case using the leading nozzle. It becomes clear that as a result of gas modulation, the melting pool experiences an impulse every 10 ms, which leads to changes in weld penetration geometries in total. The additional analyses of the recorded processes, which are using digital image processing, allow initial assumptions to be made on how the gas pulse affects the melt and thus the process. It also allows initial interpretations of the cause of the change in the weld geometry. For the evaluation of the test welds with and without gas pulse, the behaviour of the elliptical surface of the melting zone (A) over the time is used as an evaluation criterion. It can be seen that the process calms down considerably due to a instationary gas flow compared to a stationary gas flow (see Figure 7).

If the stationary gas flow still generates strong turbulences in the melt pool and thus forces the melt to expand in width and length – the arithmetic mean of the area size is approx. 2500 µm² with a standard deviation of up to 850 µm². The modulation of the gas flow with a frequency of f_Puls =100 Hz succeeds in significantly limiting the fluctuations of the ellipse area. The derived mean value drops to about 1100 µm² ± 130 µm². This is also expressed by the comparison of the images on the top of the seam in Figure 8. While the seam scaling under stationary conditions (Figure 8(a)) still appears very uneven, with a very unsteady bead-like progression at the seam edges, the use of an instationary flow (Figure 8 (b)) reveals a finer scaling of the seam surface with an even progression along the seam edges. This effect is entirely due to the instationary process gas flow.

4.0 DISCUSSION

The metallographic analysis of the produced samples showed that the seam width values when using a instationary gas flow lagged behind those under stationary conditions. A possible explanation for this, apart from the influence of the changing dynamic pressure or the force of the gas flow acting on the melt pool, is the change in the Marangoni flow in the melt pool itself. This phenomenon, which occurs as a result of the increase in oxygen content, is described by the Heiple-Roper theory [14] [15] [16].

Since the parameters with gas pulse for the test series are chosen in such a way that no volume flow of the protective gas argon prevails in the base current phase, this could mean that during this period, the protective gas successively decreases and the ambient medium (air) influences the melt.

Due to the increase of the oxidising gas during the process, a change in the Marangoni flow would occur. This is accompanied by a change with regard to the weld penetration characteristics, as there is a change in the temperature gradient ($\frac{\delta\sigma}{\delta T}$) of the surface tension from negative to positive. As a result, there is a reversal of the Marangoni flow from the edge of the melt pool to the centre. The hotter material is now forced downwards and colder material from the peripheral areas flows in. The result is narrow and deeper seams.

At the same time, the maximum dynamic pressure changes. The simulation is performed by changing the base flow $\dot{V}_\mathrm{G}$, but currently it is not possible to simulate a pulsating flow of the shield gas in Flow3D®. It can be shown that the dynamic pressure under instationary conditions is about one power of ten lower than under stationary

[C] Determined during the preliminary tests by multiple welds with the same parameter set

conditions, depending on the pulse frequency. The following consideration can be derived from this: Assuming an almost identical footprint, as a result of the laser and machine parameters being kept constant between the experiments, there is a significant reduction in the force acting on the melt pool. Likewise, the modulation of the gas drastically reduces the time the force acts on the melt. The minimisation of these two factors causes a reduction in the size of the impulse and this means a reduction in the vertical and horizontal deflection of the melt. This could be compared to air currents of different strengths hitting water surface and thus causing an uneven displacement of the medium towards the edges[D]. The "bundling" of the molten surface that occurs in this way could not only result in a reduction of the seam width, but also an increase in the intensity of the laser radiation at

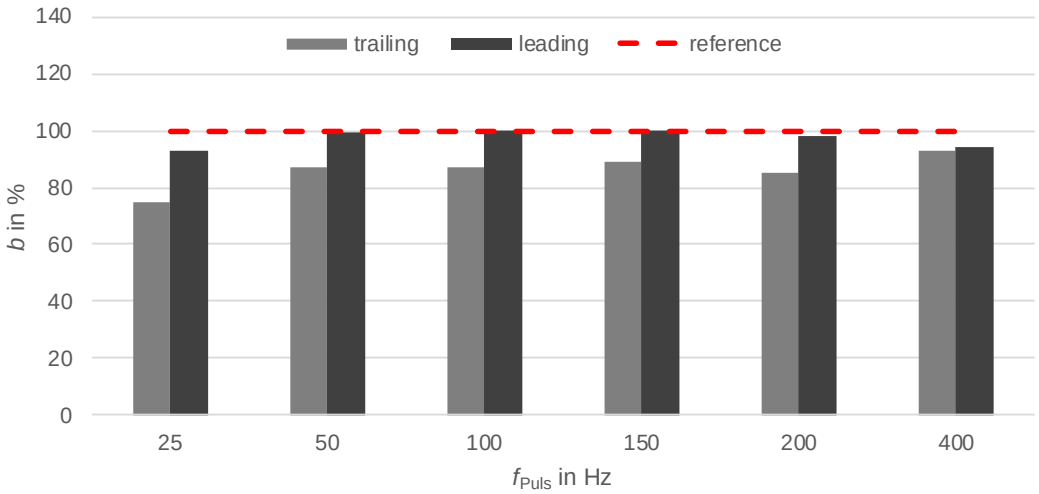

(a)

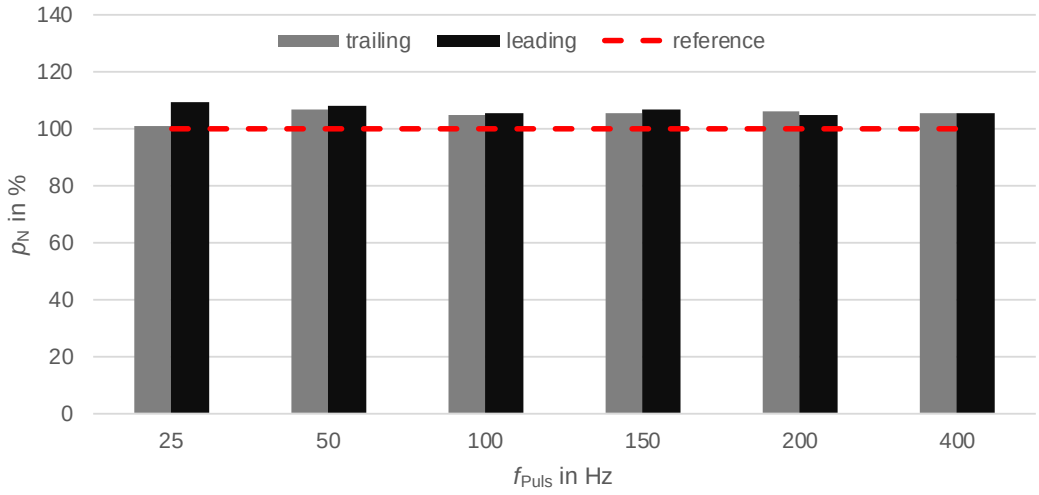

(b)

Figure 12. Representation of the weld penetration characteristics (seam depth [p_N; picture b] and seam width [b; picture a]) when using instationary gas flows as a function of the pulse frequency (f_{Puls}) and the nozzle position (trailing/leading) related to the parameter set without gas pulse (reference parameter set ≡ 100 %, red line)

the processing location and thus an increase in temperature would be the direct consequence of the instationary gas flow. By maximising I_L and T in this way, the process energy is introduced deeper into the component and an increase in the seam depth occurs.

For the time being, it remains to be noted that there is a directional dependency with regard to the formation of the weld seams and the arrangement of the shielding gas nozzle, which results in different aspect ratios. Furthermore, the use of modulated gas flow seems to make it possible to adjust the aspect ratios from trailing to leading shielding gas nozzle, which can be advantageous with regard to direction-dependent welding.

[D] The flow behaviour of the melt of metals is similar to that of water [18] [17].

By using the technology to modify the process gas flow, three new parameters are available for the user to influence the results of laser material processing: The pulse frequency (f_{Puls}) as well as the volume flows of the shielding gas in the pulse ($\dot{V}_{\mathrm{P}}$) and base current phase ($\dot{V}_{\mathrm{G}}$). The effect on the welding result due to a changed pulse frequency can be derived from the diagrams in Figure 12.

Starting from a parameter set without gas pulse, which in the context of the evaluation takes the value 100 %, the results of the welds produced with instanionary gas flow are in a specific relation to these. Thus, by means of continuous gas pulses at different pulse frequencies ($1\ \mathrm{Hz} < f_{\mathrm{Puls}} < 400\ \mathrm{Hz}$), it is possible to vary the seam width and depth significantly with otherwise constant parameters. Depending on a nozzle position trailing the process, width (by ≈ 10 %) can be significantly reduced in relation to the reference sample. At the same time, the welding depth experiences an increase of approx. 5 %. When changing the nozzle position to an arrangement ahead of the process, changes in the weld-in characteristics also occur due to the modification of the pulse frequency. Here, too, the weld width of the samples can be reduced by ≈ 2 % in relation to the reference samples, while the weld penetration depth increases in percentage terms (≈ 5 %). The explanation for this type of influence on the seam or for the change in the seam characteristics due to the new parameters can be found in the effects formulated by the Heiple-Roper theory. On the other hand, it is the changes in dynamic pressure and the associated variation in the forces acting on the melt pool that have a direct influence on the design of the specific seam geometry. Thus, with regard to the effect on the behaviour of laser beam welds by the parameters provided by the gas pulse technology, it can be stated that a change in the results is possible through the variables f_{Puls}, $\dot{V}_{\mathrm{P}}$ and $\dot{V}_{\mathrm{G}}$. By skilfully adjusting and combining the newly obtained parameters, as well as in combinations with the already existing parameters, the formation of the weld seam can be modified not only in terms of width and depth, but also in terms of the optical component, which means finer seam surface.

5.0 CONCLUSION AND FUTURE RESEARCH

In the field of industrial manufacturing, laser processes is a key technology – highly precise and extremely fast. A wide range of parameters makes it possible to realise different applications with high quality and quantity. The greater the possibility of influencing the process through the choice of different parameters, the more precisely it is possible to react to disturbance variables and bring the expectation into better harmony with the result. This also applies to the process of joining by means of laser radiation. By adjusting variables such as laser power, focus position or feed rate, perfect seams can be produced with minimal heat input.

By integrating technology for generating temporally alternating (pulsed) gas flows, the user has new, additional parameters at his disposal, such as the pulse frequency, different volume flows in the pulse and base flow phases or a freely selectable switching ratio between the phases, in order to positively influence the joining process and thus the result. Based on Thurner's [3] and Ebert's [4] dissertations, the main focus is on the technical realisation of this technology in relation to laser systems, which mainly refers to the prevailing higher process speeds and the associated maximum pulse frequency ($f_{\mathrm{Puls}} \leq 300\ \mathrm{Hz}$).

This being said, the implementation implied specific adaptations of the three core elements - actuator, measuring section, control – or a completely new conception of the technology structure. The previously used actuators are replaced by more powerful proportional valves in order to maximise the achievable cut-off frequency and thus possible process speeds. Furthermore, the measuring section for recording specific controlled variables is optimised for the new conditions. By using so-called Venturi tubes, it is now possible to generate pressure differences without creating disturbing turbulences within the flow. Thus, the measuring accuracy of the system could be significantly improved. The computer-based control logic is also adapted. This included the transfer of the control to a new software platform, combined with the revision of the entire programming.

The investigations carried out included the analysis of the effect of specific parameters of transient gas flows on the dynamic pressure. The main focus is on determining the influence of the pulse frequency and the volume flows in the pulse and base flow phases on the shape and behaviour of the flow. The results are compared with the results of tests under steady-state flow conditions, whereby requirements for the design of the system components of the gas pulse technology as well as essential boundary conditions could be derived and subsequently technically implemented.

The subsequent integration of gas powder technology into different laser processing systems and the performance of investigations into the joining of materials using unsteady gas flows demonstrated the potential of the technology. Based on reference samples - welded without modulated gas flow - the results of the seams produced with modulated gas flow stand in a specific relation to them. Just by varying the parameters of the new technology, the weld-in characteristics could be significantly changed. As a result of the cyclical change in the process gas flow, the associated variation in the prevailing shielding gas composition and the dynamic pressure acted on the melt, which imposes a defined movement on the melt; thus, it is possible to achieve:

- increase of the welding depth by up to 5 %,
- minimise the seam width by approx. 10 %, and

- influence the seam height in such a way that changes of ± 20 % are achieved depending on whether the shielding gas nozzle followed or preceded the process.

Although the effects/possibilities arising from the use of the gas pulse technology have only been investigated in rudimentary form within the scope of this work, they nevertheless clearly demonstrate the efficiency of this technology.

In addition to the pulse frequency (f_{Puls}) and the volume flow rates of the protective gas in the pulse ($\dot{V}_{\mathrm{P}}$) and base flow phase ($\dot{V}_{\mathrm{G}}$), there are other system-specific parameters that influence the process and the results. This is mainly to be seen with regard to a variation of the pulse shape as well as the adjustment of the pulse lengths and intervals (change of the switching ratio). In order to grasp the full scope of the technology and apply it industrially, the investigation into the way in which these parameters are affected holds great scientific potential. The same applies to investigations that use at least two different gases in the pulse and base flow phases, with the aim of allowing different chemical elements to react alternately with the melt and thus achieve mechanical-technological improvements in the weld. Furthermore, it is conceivable to extend the application possibilities of the technology to other areas of laser material processing and to investigate their influence in more detail. In relation to the sub-areas of "cutting" and "coating", improvements in the quality of the cut edge could result from a transient change in the melt film thickness that is formed. An increase in the homogeneous distribution of hard material particles within the solidifying melt could also occur, which would result in an improvement in the wear properties.

Parallel to all these welding investigations, the film and photographic technology used as well as the algorithms for digital image processing must be modified and verified for a high-resolution analysis of the processes. The data sets obtained in this way, combined with the results from the metallographic investigations, form the basis for the further development of the process simulation to investigate possible effects occurring when using a transient gas flow in the field of laser material processing.

ACKNOWLEDGEMENT

We would like to thank the staff of the Chair of Welding Engineering and the Media Computing Junior Professorship at Chemnitz University of Technology and the Fachgebiet Hybride Fertigung at Brandenburg University of Technology for their commitment to this research project.

REFERENCES

[1] T. Ramge, “Offen für Innovation – Das Wunderwerkzeug,” 2005. [Online]. Available: https://www.brandeins.de/magazine/brand-eins-wirtschaftsmagazin/2005/erkenne-die-moeglichkeiten/das-wunderwerkzeug. [Accessed 5. January 2021].

[2] E. U. Beske, Untersuchungen zum Schweißen mit kW Nd:YAG-Laserstrahlung, vol. 257, Düsseldorf: VDI-Verlag GmbH, 1992.

[3] S. Thurner, Erzeugung und Anwendung modulierter Prozessgasströme beim Schutzgasschweißen, Chemnitz: TU Chemnitz, 2008.

[4] L. Ebert, Beeinflussung von geschweißten Auftragschichten durch instationäre Gasströme im Plasma-Pulver-Schweißprozess, Chemnitz: TU Chemnitz, 2011.

[5] B. John, Verwendung instationärer Gasströme in der Laserfügetechnik, vol. 6 Wissenschaftliche Schriftenreihe CHEMNITZER FÜGETECHNIK, Chemnitz: TU Chemnitz, 2018.

[6] F. U. Mathiak, Ebene Flächentragwerke II - Grundlagen der Plattentheorie, Neubrandenburg: Hochschule Neubrandenburg, 2008.

[7] E. Truckenbrodt, Fluidmechanik – Band 2: Elementare Strömungsvorgänge dichteveränderlicher Fluide sowie Potential- und Grenzschichtströmungen, 4. Auflage ed., Berlin: Springer-Verlag, 1999.

[8] *DIN EN ISO 5167 - Durchflussmessung von Fluiden mit Drosselgeräten in voll durchströmten Leitungen mit Kreisquerschnitt*, Berlin: Deutsches Institut für Normung e. V., 2004.

[9] F. Brall, “Regelungen,” [Online]. Available: https://rn-wissen.de/wiki/index.php/Regelungstechnik# PID-Regler. [Accessed 01. March 2021].

[10] Institut für Physik Universität Augsburg, “Physikalisches Praktikum für Fortgeschrittene – PID-Regler,” [Online]. Available: http://www.physik.uni-augsburg.de/~sausemar/FP14/FP14. [Accessed 20. January 2014].

[11] U. Köhler, “Device for processing workpieces by laser radiation – uses turbine wheel to circulate gas at high speed, and optically monitors outlet valve”. Patent DE3927451, July 1990.

[12] B. John, D. Markert, N. Englisch, M. Grimm, M. Ritter, W. Hardt and D. Kowerko, “Quantification of geometric properties of the melting zone in laser-assisted welding,” in *Lasers in Manufacturing Conference 2017*, München, 2017.

[13] D. Kowerko, M. Ritter, R. Manthey, B. John and M. Grimm, “Quantifizierung der geometrischen Eigenschaften von Schmelzzonen bei Laserschweißprozessen,” Forum Bildverarbeitung 2016, 2016.

[14] K. C. Mills, “The importance of materials properties in high-temperature processes,” *3rd international slag valorisation symposium,* pp. 69-85, 2013.

[15] B. J. Keene and R. F. B. K. C. Mills, “Surface properties of liquid metals and their effects on weldability,” *Materials Science and Technology,* pp. 568-571, 1985.

[16] A. A. Shirali and K. C. Mills, “The effect of welding parameters on penetration in GTA welds,” *Welding Research Supplemnet,* pp. 347-353, 1993.

[17] B. Bochtler, O. Gross, I. Gallino and R. Busch, “Thermo-physical characterization of the Fe67Mo6Ni3.5Cr3.5P12C5.5B2.5 bulk metallic glass forming alloy,” *Acta Materialia,* no. 118, pp. 129 - 139, 2016.

[18] R. Jenning, Rheologisches Verhalten teilerstarrter Metalllegierungen, Technische Universität Erlangen, 2009.